Effect of the altitudinal variation of the gravitational acceleration on the thermosphere simulation

Yue Deng,[1] Aaron J. Ridley,[2] and Wenbin Wang[1]

Received 6 February 2008; revised 18 April 2008; accepted 3 June 2008; published 4 September 2008.

[1] For simplicity, a constant gravitational acceleration ($\vec{g}$) is assumed in many general circulation models (GCMs). To estimate the influence of the altitudinal variation of the $\vec{g}$ on the thermosphere simulation, two runs have been made under the solar maximum condition using the non-hydrostatic Global Ionosphere Thermosphere Model (GITM), including one with a constant $\vec{g}$ (8.7 m/s^2) and the other with an altitude-dependent $\vec{g}$. During geomagnetic quiet time, globe averagely, the constant $\vec{g}$ case overestimates the neutral density by 30% and underestimates the temperature by 10% around 120 km altitude compared with the altitude-dependent gravitation case. A post-processing then has been done to the constant $\vec{g}$ case by shifting the atmosphere vertically according to the altitude-dependent $\vec{g}$. After this shifting, the global average density difference decreases to 10%, and the temperature difference also changes correspondingly to 2% at 120 km. The $\vec{g}$ specification directly causes the vertical shift of the atmosphere through changing the scale height. Meanwhile, it changes the temperature profile, which feeds back to the altitude profile of the neutral density. In order to separate these two effects, three simple tests with one-dimensional semi-realistic atmosphere have been conducted, and the primary results are that the vertical shifting and the temperature variation caused by the $\vec{g}$ specification contribute 20% and 25% of the density difference, respectively. This study gives a reference to other GCMs about the validity of the constant gravitational acceleration assumption.

Citation: Deng, Y., A. J. Ridley, and W. Wang (2008), Effect of the altitudinal variation of the gravitational acceleration on the thermosphere simulation, *J. Geophys. Res.*, *113*, A09302, doi:10.1029/2008JA013081.

1. Introduction

[2] The thermosphere is a complex and externally-forced deterministic system [*Forbes*, 2007]. These forces include solar EUV radiation [*Rishbeth et al.*, 2000], high-latitude electrodynamics [*Killeen and Roble*, 1988], particle precipitation [*Akasofu*, 1976] and waves propagating from the lower atmosphere [*Hines*, 1967]. In the last several decades, many modeling efforts have been made to improve to our understanding of this complex thermosphere system. Some of the well-known global thermospheric models are the Thermosphere Ionosphere Electrodynamic General Circulation Model (TIEGCM) and its predecessors [*Richmond*, 1992; *Roble et al.*, 1988; *Dickinson et al.*, 1984, 1981], Coupled Thermosphere Ionosphere Model (CTIM) [*Fuller-Rowell and Rees*, 1980, 1983; *Rees and Fuller-Rowell*, 1988, 1990].

[3] In many GCMs, the gravitational acceleration ($\vec{g}$) is set to be a constant in a hydrostatic atmosphere. With this assumption, the column mass density between two pressure levels (ΔP) is constant ($\rho \Delta z = -\frac{\Delta P}{g}$), where ρ is the mass density and Δz is the altitude difference between two pressure levels. The continuity equation in the pressure coordinates can be simplified as the divergence of the velocity ($\vec{U}$) equals to zero ($\nabla \cdot \vec{U} = 0$) [*Holton*, 1992] assuming hydrostatic equilibrium and constant gravity. The constant $\vec{g}$ assumption is valid in the low-middle atmosphere models since the vertical extent of the low-middle atmosphere is only several tens of kilometers, resulting in only a 1% error in the specification of $\vec{g}$. However, in the upper atmosphere, where the altitude range covers several hundred kilometers (100–500 km), the decrease of the gravitational acceleration with altitude may not be negligible, and can impact the thermosphere through changing the scale height ($H = \frac{kT}{mg}$, where k is the Boltzmann constant, T is the temperature, m is the mean molecular mass and g is the gravitational acceleration). In order to more accurately simulate the thermosphere, an altitude-dependent $\vec{g}$ should be used in GCMs. However, it may not be easy for the models using pressure coordinates to change to the altitude-dependent $\vec{g}$, since the mass conservation between pressure levels would not be valid any more and the continuity equation would need to be reformulated [*Holton*, 1992]. Therefore it is very important to evaluate how strongly the constant gravitational acceleration specification can affect the thermospheric simulations. This may be a significant source of discrepancy when conducting neutral density

[1] High Altitude Observatory, National Center for Atmospheric Research, Boulder, Colorado, USA.
[2] Center for Space Environment Modeling, University of Michigan, Ann Arbor, Michigan, USA.

0148-0227/08/2008JA013081

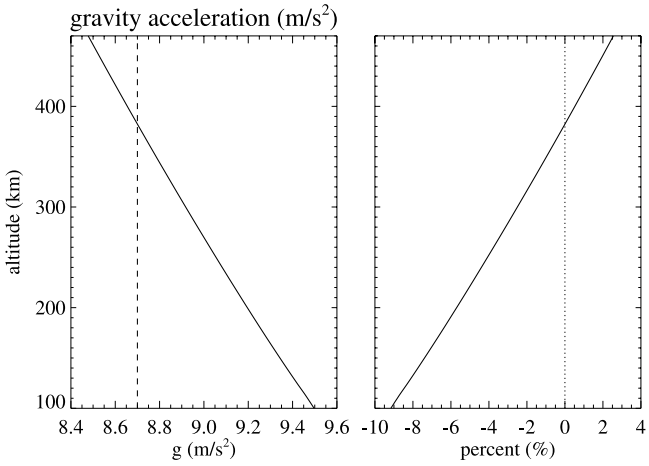

Figure 1. Left: Altitude variation of the gravitational acceleration (m/s^2). Solid: altitude-dependent gravitational acceleration; dash: constant gravitational acceleration. Right: Percentage difference between the altitude-dependent g and the constant g ($\frac{g_{const}-g_{dependent}}{g_{const}} \times 100\%$).

data-model comparisons, since there may be a systematic error when $\vec{g}$ is assumed to be a constant throughout the thermosphere. Some non-hydrostatic thermospheric models using a variable $\vec{g}$ are available in the community [*Chang and St.-Maurice*, 1991; *Ma and Schunk*, 1995; *Demars and Schunk*, 2007]. However, they are either a 2-D model [*Chang and St.-Maurice*, 1991], or without a self-consistent ionosphere [*Ma and Schunk*, 1995; *Demars and Schunk*, 2007]. In this study, using the newly developed non-hydrostatic Global Ionosphere Thermosphere Model (GITM) in altitude coordinates, the influence of the altitudinal variation of $\vec{g}$ on thermospheric simulations has been investigated under different geomagnetic conditions.

2. Model Description

[4] GITM is a 3-dimensional spherical code that models the Earth's thermosphere and ionosphere system using a stretched grid in latitude and altitude [*Ridley et al.*, 2006]. It is a non-hydrostatic model with variable gravity acceleration. GITM relaxes the hydrostatic equilibrium condition on the thermosphere, allowing non-hydrostatic phenomena to form due to non-gravitational forces [*Deng et al.*, 2008]. The most relevant feature of GITM for this study is that GITM solves on an altitude grid, allowing $\vec{g}$ to change with height, instead of solving on a pressure grid with a constant $\vec{g}$. GITM has been used to investigate vertical ion flows [*Deng and Ridley*, 2006b], Joule heating [*Deng and Ridley*, 2007] and thermospheric neutral winds [*Deng and Ridley*, 2006a]. The spatial resolution for this study is 5° longitude by 5° latitude (the same as the TIEGCM) by 1/3 scale height, and the temporal resolution is approximately 2 seconds. The lower boundary condition at 97 km altitude for the thermosphere is specified by the MSIS model [*Hedin*, 1987].

[5] For simplicity, the gravitational acceleration is assumed to be constant (e.g., 8.7 m/s^2 in the TIEGCM) at the thermosphere altitudes in most hydrostatic models. However, in reality, $g = \frac{GM_E}{(R_E+Z)^2}$, where G is the universal gravitation constant, M_E is the mass of the Earth, R_E is the radius of the Earth and Z is the altitude. The gravitational acceleration decreases with altitude, as shown by the solid line in Figure 1 (left). g is equal to 9.5 m/s^2 at 100 km altitude, which is 9% larger than 8.7 m/s^2. However, at 500 km altitude, g is close to 8.45 m/s^2, which is close to 3% smaller than 8.7 m/s^2. Since the scale height has an inverse relationship with g, one would expect that using a constant, instead of an altitude-dependent, gravitational acceleration may result systematic differences in the simulated thermosphere density and temperature distributions. In GITM, it is easy to force gravity to be a constant value. For this study, we have run GITM for the Halloween storm (29–31 October 2003) with both a constant and a realistic gravity profile to determine the effects of a constant gravity assumption.

3. Results

[6] The impact of the gravitational acceleration on the global mean density and temperature in solar maximum ($F10.7 = 250 \times 10^{-22}$ W/m^2/Hz) during a relatively quiet time period is investigated first. 0600 UT on 29 October 2003, when the interplanetary magnetic field (IMF) B_z was −2.5 nT (Kp = 4), was a relatively geomagnetic quiet time compared with the following Halloween storm as shown in Figure 2. Figure 3a (left) shows the globally averaged density, when GITM was run with an altitude-dependent gravity (solid black line) and a constant gravity equals to 8.7 m/s^2 (dashed red line). Figure 3a (right) shows the global average (solid), minimum (left dashed) and maximum (right-dashed) percentage differences of density between the two runs ($\frac{\rho_{const}-\rho_{dependent}}{\rho_{const}} \times 100\%$) as a function of altitude. The global average density percentage difference is close to 30% at 120 km, and the minimum and maximum

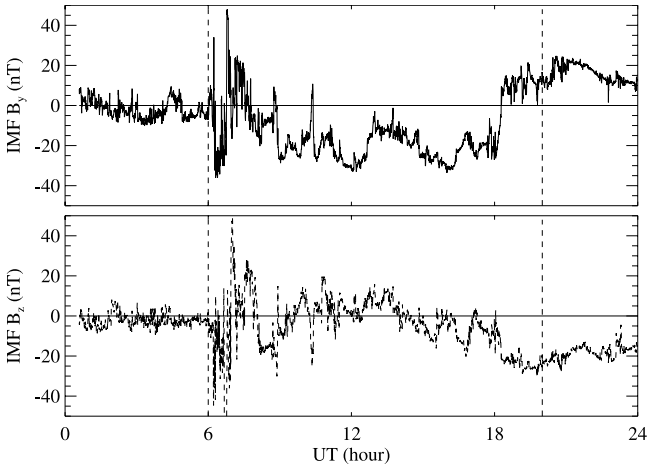

Figure 2. The temporal variation of the Interplanetary Magnetic field (IMF) condition during 29 October 2003 observed by the Advanced Composition Explorer (ACE) satellite. The vertical dashed lines mark 0600 UT and 2000 UT, which represent the geomagnetic quiet time and geomagnetic active time in this study, respectively.

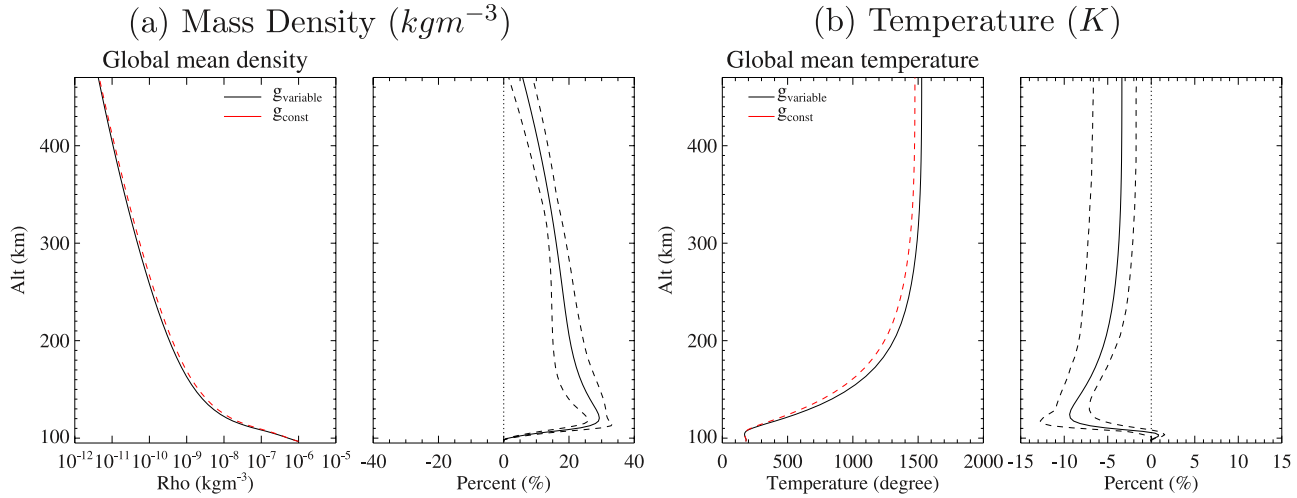

Figure 3. (a) Comparison of the global mean mass density when using different gravitational acceleration. (left) Altitude profiles of the global average density with the altitude-dependent gravitational acceleration (black solid line) and the constant gravitational acceleration (red dash line) at a geomagnetic quiet time (0600 UT, 29 October 2003). (right) Percentage difference of the constant gravitation case from the altitude-dependent gravitation case, solid line for the global mean and dashed lines for the minimum and maximum percentages, respectively. (b) Same as Figure 3a except for the temperature.

mass density percent differences are approximately 5% away from the mean percentage difference at all altitudes. Therefore the localized difference can be 25% to 35%. The reason for the positive mass density difference is that below 380 km, $|g_{const}| < |g_{dependent}|$ so the gravity exerts a smaller force on the atmosphere in the constant gravity case, resulting in a weaker gradient in pressure, allowing the atmosphere to expand. Therefore, at a specific altitude, the density with constant $\vec{g}$ is larger than that with altitude-dependent $\vec{g}$. As shown in Figure 1, the largest difference of gravitational acceleration happens at the bottom, but Figure 3a shows that the density difference at the bottom is close to zero. This is because the low boundary conditions for the neutral densities are specified by the MSIS empirical model [*Hedin*, 1987] and are identical in the two cases with different $\vec{g}$. Several scale heights are needed to build up the density difference caused by the gravitational acceleration assumption. The position of the density difference peak (120 km) is coincident with the position of the temperature difference peak. Above 380 km altitude, $g_{const} > g_{dependent}$ as shown in Figure 1, however Figure 3a shows that ρ_{const} is still larger than $\rho_{dependent}$. The reason for this is that the density, $\rho = \rho_0 e^{\int -\frac{dz}{H}}$ where ρ_0 is the mass density at the lower boundary, depends on the integrated scale-heights below. Therefore it would take many scale heights to result in ρ_{const} being smaller than $\rho_{dependent}$.

[7] The impact of gravitational acceleration on the global average neutral temperature is shown in Figure 3b. The constant case has a lower temperature than the altitude-dependent case, and the global average percentage difference reaches 10% around 120 km altitude. The maximum and minimum percentage differences are about 3% away from the mean difference. The difference in temperature between the two simulations can be explained as the result of the inverse relationship between the temperature change rate and the density when assuming the total absorbed energy in the thermosphere is the same ($dT/dt \sim Q/\rho$, where Q is the total heating and ρ is the total mass in the thermosphere). It means that if the same amount of energy is deposited into two atmospheres, one with less density then the other, that one would be heated up more than the other. This temperature difference modifies the scale height, resulting in a nonlinear coupling between the gravity and density.

[8] The scale height depends on temperature, mean molecular mass and gravitational acceleration, therefore $\frac{dH}{H} = \frac{dT}{T} - \frac{dm}{m} - \frac{dg}{g}$, which means that the percentage variations of temperature, mean molecular mass and gravitational acceleration are equally important to the percentage variation of the scale height. Since the gravity acceleration, temperature and mean molecular mass are coupled together, the 9% to −3% difference in gravitational acceleration (shown in Figure 1) causes 3% difference in temperature above 200 km altitude (shown in Figure 3) and less than 1% difference in mean molecular mass at all altitudes (not shown). The temperature and mean molecular mass differences feed back to the neutral density profiles. Since GITM is a self-consistent coupled model, these feedbacks have already been automatically included in the results shown in Figures 3, 4 and 5. Due to the small magnitude of the percentage difference of mean molecular mass, we only discuss the feedback of the temperature variation in this study.

[9] It should be noted that in some hydrostatic models, the altitudinal variation of the gravitational acceleration is taken into account in post-processing, when calculating the altitudes of the pressure levels. Therefore a similar post-processing is done to the constant gravity case here by shifting the atmosphere vertically according to the altitude-dependent gravitational acceleration. When assuming the

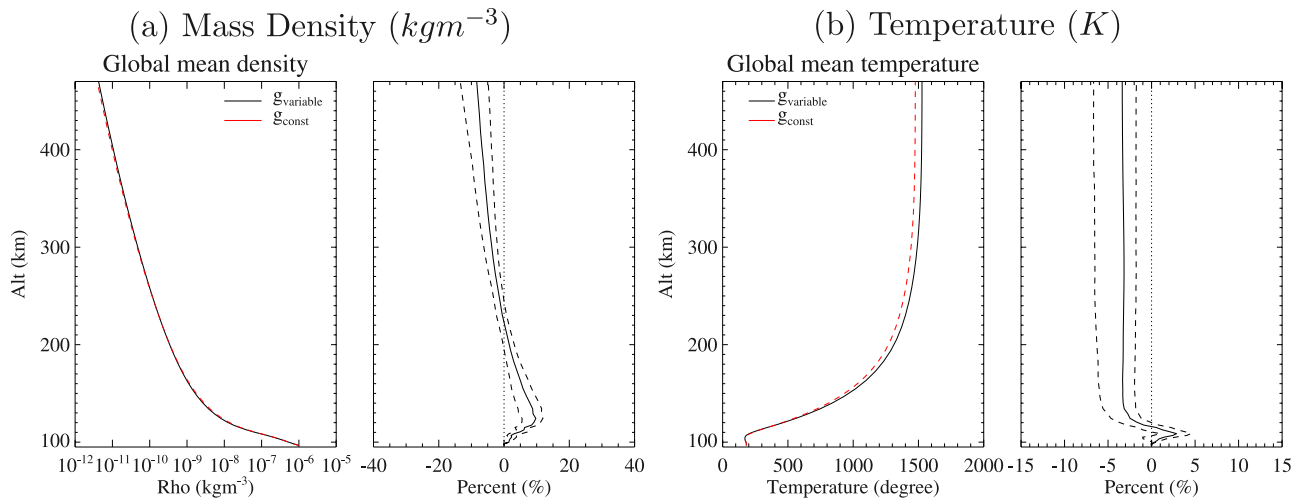

Figure 4. Same as Figure 3, except that the atmosphere has been shifted according to the altitude-dependent $\vec{g}$ in the constant gravitation case.

system to be hydrostatic ($\frac{\Delta P}{\Delta z} = -\rho\, g$) and using the ideal gas law ($p = \rho\, \frac{kT}{m}$),

$$\Delta(\ln P) = -\frac{mg}{kT} \cdot \Delta z, \tag{1}$$

where Δz and $\Delta(\ln P)$ are the vertical distance and the difference of the log pressures between two pressure levels, respectively. It is assumed that the shifting just physically moves the atmosphere in the vertical direction and does not change the state of the gas parcel, (i.e., $P_1 = P_2$, $m_1 = m_2$ and $T_1 = T_2$, where the subscript "1" and "2" represent the conditions before and after the shift, respectively). Utilizing this, a relationship between Δz_1 and Δz_2 is derived:

$$\Delta z_2 = \Delta z_1 \frac{g_1}{g_2} \tag{2}$$

where g_2 is the altitude-dependent gravitational acceleration, g_1 is the constant gravitational acceleration, and Δz_1 and Δz_2 are the distance between pressure levels with the constant $\vec{g}$ and the altitude-dependent $\vec{g}$, respectively. While an assumption is made on the change of atmospheric state during the shift, there was no constraint made on the actual profiles as a function of pressure level. Equation (2) shows that when $g_2 > g_1$, $\Delta z_2 < \Delta z_1$, meaning that the pressure levels and the atmosphere move downward when g is large. Models such as the TIEGCM utilize equation (2) to shift altitude levels in a post-processing technique. This allows more consistent comparisons to measurements at specific altitudes. To test this shifting, the GITM results utilizing constant gravity are shifted according to the altitude-dependent gravitational acceleration as described above.

[10] Figure 4a shows the comparison between the shifted constant gravity case and the altitude-dependent case. After shifting, the global average percentage difference in the density decreases from 30% to 10% at 120 km altitude. The shifting over compensates results above 200 km and makes the percentage difference of the mass density negative.

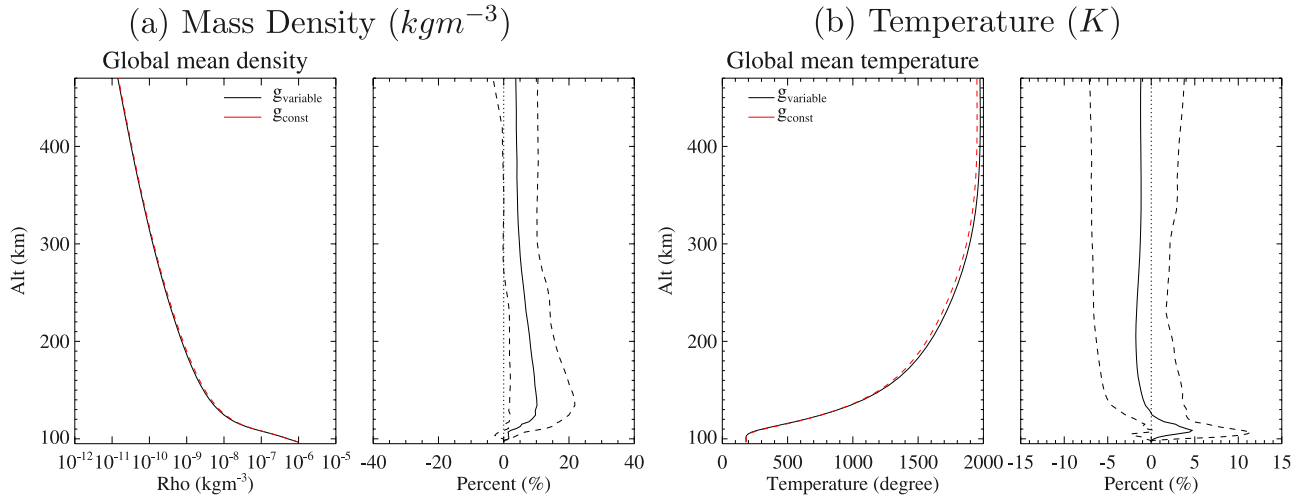

Figure 5. Same as Figure 4 except during a geomagnetic active time (20 UT, 29 October 2003).

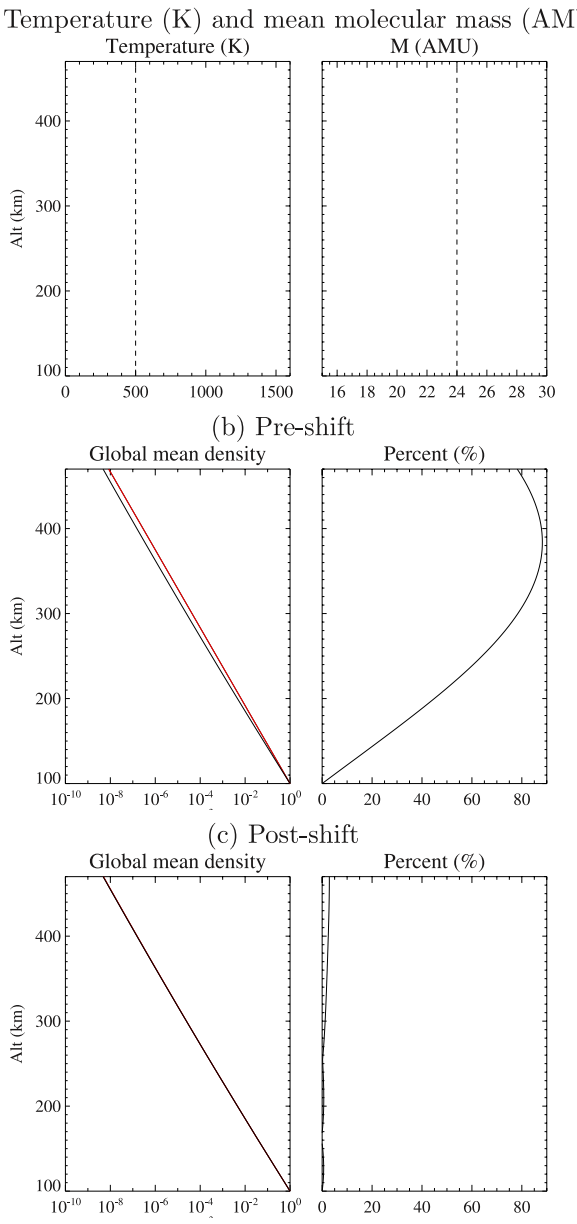

Figure 6. Simple test 1 in a one-dimensional semi-realistic atmosphere for the constant temperature (T) and mean molecular mass (M) condition. (a) Altitudinal distribution of T and M. (b) Altitudinal distribution of mass density for the constant gravity case (black line) and altitude-dependent case (red line), and the percentage difference between these two cases. (c) Same as Figure 6a except that the constant case has been shifted according to the altitude-dependent gravitational acceleration.

Figure 4b shows that the percentage difference in the temperature also changes correspondingly. At 120 km, the global average temperature difference changes from −10% to −2%. However, above 200 km altitude, the percentage difference stays at −3% and changes little with the shift, since the atmosphere is almost isothermal above this altitude. The shift results in a positive temperature difference peak at 110 km, which is most likely due to the fixed lower boundary condition and may not be physically realistic. The significant reduction of the density difference after shifting the solution shows that one primary effect of the altitudinal variation of $\vec{g}$ is to shift the atmosphere vertically. Meanwhile, the persistent 3% temperature difference caused by the altitudinal variation of $\vec{g}$ also strongly changes the density profile. However, the shifting and the temperature variation do not totally remove the density difference, which implies that there are some other effects of the altitudinal variation of $\vec{g}$ on the density and temperature profiles. Because the thermosphere-ionosphere is a self-consistent coupled non-linear system, the varied density and temperature profiles change the distribution of the solar irradiation absorption, neutral wind circulation and thermal conductivity, which in turn feeds back to alter the temperature and density distribution. Meanwhile, the $\vec{g}$ affects the ionosphere, which also feeds back to the thermosphere neutral winds and neutral temperature through processes, such as ion drag and Joule heating.

[11] Similar runs have also been done for the geomagnetic active time (2000 UT, 29 October 2003) to show the dependence of the gravitational acceleration effect on geomagnetic conditions. As shown in Figure 2, the IMF B_z was close to −20 nT at 2000 UT, which typically represents a geomagnetic active condition. Figure 5 shows the global mean density and temperature profiles for the shifted constant case and altitude-dependent case at 2000 UT. The average density percentage difference increases more at high altitudes than at low altitudes when compared with the geomagnetic quiet time (Figure 4). The deviation amplitude (half of the minimum-maximum difference) is 5−10% and larger than that in the geomagnetic quiet time (3−5%). The average percentage difference in temperature is smaller in the geomagnetic active time than in the geomagnetic quiet time, since the absolute value of the temperature increases with the activity level. The deviation amplitude of the temperature percentage difference is approximately 5%, which is almost twice as large as that in the geomagnetic quiet time (3%). The increase of the deviation amplitude indicates that the density and temperature differences caused by the gravitational acceleration have more spatial structure and localized variation during geomagnetic active time than geomagnetic quiet time.

4. Discussion

[12] The altitudinal variation of $\vec{g}$ affects the neutral density profile primarily in two ways, either directly shifting the atmosphere vertically through changing the scale height, or varying the temperature, which feeds back to the neutral density profile. In order to separate these two effects, three simple tests have been conducted in a one-dimensional semi-realistic atmosphere, in which the density is simply calculated using $\rho = \rho_0 e^{\int -\frac{dz}{H}}$, where ρ is the density, ρ_0 is the density at the lower boundary and set to be 1, z is the altitude and H is the scale height. As shown in Figures 6a, 7a and 8a, these three tests include: (1) constant temperature (T) and mean molecular mass (M), (2) altitude-dependent T and M, and (3) the same as (2) except that T is reduced by 3% in the constant gravity case (minicing the trends observed in the modeling results shown in Figure 4).

[13] In test 1 (Figure 6b), the difference between the constant case and the altitude-dependent case reaches 90%

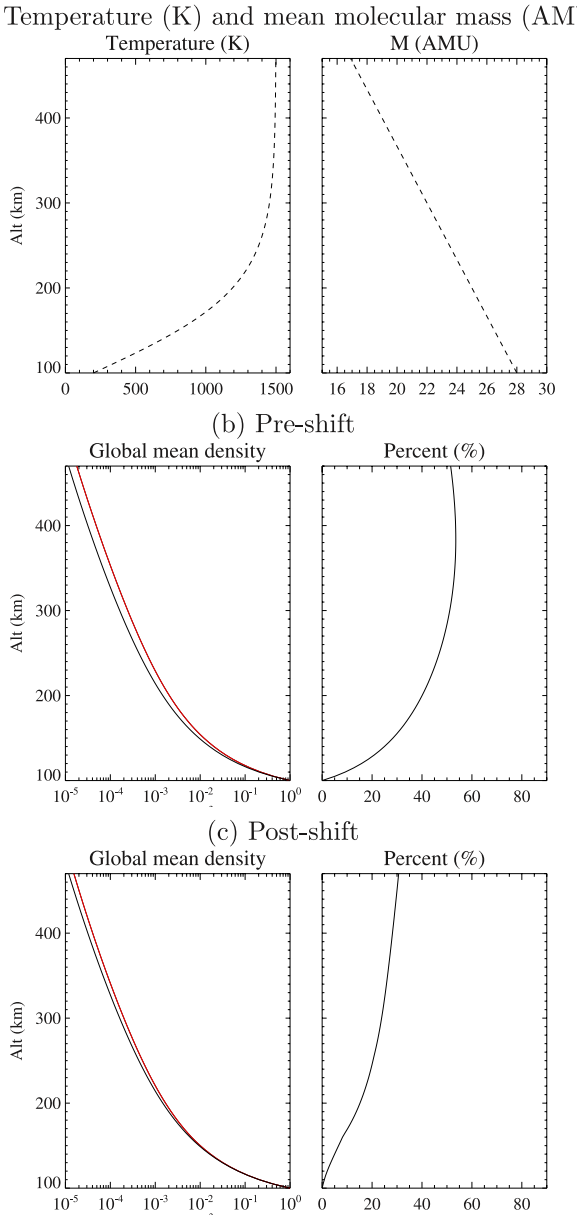

Figure 7. Test 2: Same as Figure 6 except that T and M are altitude-dependent.

around 380 km altitude, where the $g_{dependent}$ is equal to the g_{const} (8.7 m/s^2). After shifting (Figure 6c), the difference has been reduced significantly and the maximum difference is only 3%. In test 2 (Figure 7), when both T and M are altitude-dependent, the density percentage difference is close to 55% above 300 km altitude, which decreases by 25% after shifting. In test 3 (Figure 8), the impact of the gravity acceleration on the temperature profile has been considered, and the temperature is reduced by 3% in the constant case. The percentage difference of global mean density is close to 30% at 300 km, which is 25% smaller than that in test 2. The shifting then reduces it another 20% difference, as shown in the comparison between Figures 8b and 8c. In principle, test 3 is the one closest to the GITM simulation, since the non-linear temperature variation due to the gravitational acceleration and its impact on the neutral density have been automatically taken into account in the self-consistent model. However, there are some detailed differences between test 3 and GITM results shown in Figure 4, because GITM solves the physical-based dynamic equations, whereas test 3 is just calculated from a simple expression.

[14] Generally, tests 1 and 3 have the smallest percentage differences between the shifted constant case and the altitude-dependent case, as shown in Figure 6c and Figure 8c. In an idealized atmosphere with constant T and M, the shifting almost totally removes the density difference caused by the gravity acceleration specification. In a more realistic atmosphere with altitude-dependent T and M, the shifting reduces the percentage difference between the constant gravity case and altitude-dependent case by 20%. In addition, the temperature variation caused by the gravity

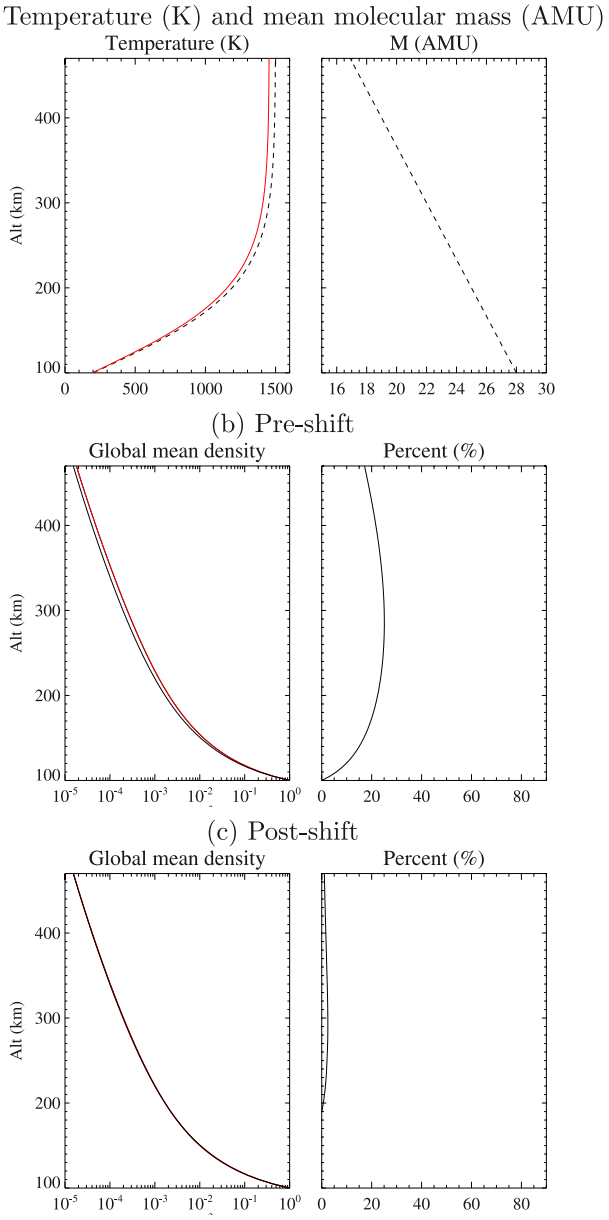

Figure 8. Test 3: Same as Figure 7 except that the temperature is reduced by 3% in the constant case.

acceleration specification also causes 25% of the density percentage difference. Therefore the effects of the shifting and the temperature variation related with gravity acceleration specification are comparable and both of them are important for the neutral density profiles. This study gives a reference to other GCMs about the significance of the gravity altitudinal variation.

5. Summary and Conclusion

[15] The gravitational acceleration has been set differently in different GCMs. In many General Circulation Models (GCMs), such as TIEGCM and CTIP, the gravitational acceleration is constant in the calculation and the altitudinal variation of the gravitational acceleration is taken into account in post-processing. Some non-hydrostatic thermospheric models using a variable $\vec{g}$ are also available in the community [*Chang and St.-Maurice*, 1991; *Ma and Schunk*, 1995; *Demars and Schunk*, 2007]. However, they are either a 2-D model [*Chang and St.-Maurice*, 1991], or without a self-consistent ionosphere [*Ma and Schunk*, 1995; *Demars and Schunk*, 2007]. In order to estimate the influence of the altitude variation of the gravitational acceleration on the thermosphere temperature and density, two runs have been made in solar maximum condition using the non-hydrostatic Global Ionosphere Thermosphere Model (GITM) under the altitude coordinates, which allow a quantification of nonlinear feedback that results when the gravity is varying with altitude instead of a constant.

[16] These runs include a constant gravitation case ($g = 8.7$ m/s^2) and an altitude-dependent gravitation case (g changes realistically with altitude). During a geomagnetic quiet time, the constant gravity simulation overestimates the globally averaged neutral density by 30% around 120 km altitude with a spread in the errors of close to 5%. The temperature decreases when a constant gravitational acceleration is used, resulting in a 10% difference around 120 km altitude. In most GCMs using the pressure coordinates, while a constant $\vec{g}$ has been used in calculation, the altitude variation of the gravitational acceleration has been taken into account during post-processing, when inferring the altitudes of the pressure levels. We have done a similar post-processing to the constant gravity case by shifting the heights of the altitude grids according to the altitude-dependent gravitational acceleration. After this shifting, the density difference has been reduced significantly and is only 10% at 120 km altitude during a geomagnetic quiet time. The temperature difference (3% above 200 km altitude) caused by the altitudinal variation of $\vec{g}$ also changes the density profile through varying the scale height. However, the shifting and the feedback of the temperature variation do not totally remove the density difference, which implies that there are some other effects of the altitudinal variation of $\vec{g}$ on density and temperature profiles. During the geomagnetic active time studied, the deviation amplitude of the percentage difference increases significantly, which means that the density and temperature differences caused by the gravitational acceleration have more spatial structure in active time. The magnitude of the temperature percentage difference is smaller during geomagnetic active time than the geomagnetic quiet time, due to the magnitude of the temperature being larger during geomagnetic active time.

[17] The altitude variation of $\vec{g}$ directly shifts the atmosphere vertically and also changes the density profile by varying the temperature. In order to separate these two effects, three simple tests have been done in a one-dimensional semi-realistic atmosphere. The results show that shifting and temperature variation cause 20% and 25% of the density percentage differences between the constant case and altitude-dependent case, respectively. Therefore both of them are important to the neutral density profiles. While the pressure level shift is a normal procedure, there is probably no simple way to include the feedback of the temperature variation in the models using a constant $\vec{g}$ and pressure level shift as a post-processing. Certain amount of the density deviation due to the temperature feedback can be unavoidable for these models. However, the value (25%) is dependent on the geomagnetic conditions and the coordinates used.

[18] When GCMs use a constant gravity, the outputs have to be post-processed to include the effect of altitude-dependent gravitation. If the pressure levels are properly shifted during a post-processing step and the feedback of the temperature variation to the density has also been taken into account, using a constant gravity term to model Earth's thermosphere and ionosphere will cause an approximately 10% error in the global average mass density. Locally the errors can grow to approximately 20% during storm periods. However, this is just a preliminary research. The quantitative results will be dependent on geomagnetic activity, solar cycle, season, etc. More detailed analysis will be meaningful and necessary, which will be investigated in a follow-up paper.

[19] **Acknowledgments.** We are grateful to Arthur D. Richmond for valuable communications and constructive comments. National Center for Atmospheric Research (NCAR) is supported by National Science Foundation (NSF). This research was also supported by NSF through grants ATM0639336 and NASA grant NN604GKL86.

[20] Zuyin Pu thanks Shun-Rong Zhang and another reviewer for their assistance in evaluating this paper.

References

Akasofu, S. I. (1976), Recent progress in studies of DMSP auroral photographs, *Space Sci. Rev.*, *19*, 169.

Chang, C. A., and J.-P. St.-Maurice (1991), Two-dimensional high-latitude thermospheric modeling—A comparison between moderate and extremely disturbed conditions, *Can. J. Phys.*, *69*, 1007–1031.

Demars, H. G., and R. W. Schunk (2007), Thermospheric response to ion heating in the day-side cusp, *J. Atmos. Sol.-Terr. Phys.*, *69*, 649–660, doi:10.1016/j.jastp.2006.11.002.

Deng, Y., and A. J. Ridley (2006a), Dependence of neutral winds on convection E-field, solar EUV and auroral particle precipitation at high latitudes, *J. Geophys. Res.*, *111*, A09306, doi:10.1029/2005JA011368.

Deng, Y., and A. J. Ridley (2006b), The role of vertical ion convection in the high-latitude ionospheric plasma distribution, *J. Geophys. Res.*, *111*, A09314, doi:10.1029/2006JA011637.

Deng, Y., and A. J. Ridley (2007), Possible reasons for underestimating joule heating in global models: E field variability, spatial resolution, and vertical velocity, *J. Geophys. Res.*, *112*, A09308, doi:10.1029/2006JA012006.

Deng, Y., A. D. Richmond, A. J. Ridley, and H.-L. Liu (2008), Assessment of the non-hydrostatic effect on the upper atmosphere using a general circulation model (GCM), *Geophys. Res. Lett.*, *35*, L01104, doi:10.1029/2007GL032182.

Dickinson, R. E., E. C. Ridley, and R. G. Roble (1981), A three-dimensional, time-dependent general circulation model of the thermosphere, *J. Geophys. Res.*, *86*(A3), 1499–1512.

Dickinson, R. E., E. C. Ridley, and R. G. Roble (1984), Thermospheric general circulation with coupled dynamics and composition, *J. Atmos. Sci.*, *41*, 205.

Forbes, J. (2007), Dynamics of the thermosphere, *J. Meteorol. Soc. Jpn.*, *85*.

Fuller-Rowell, T. J., and D. Rees (1980), A three-dimensional, time-dependent, global model of the thermosphere, *J. Atmos. Sci.*, *37*, 2545.

Fuller-Rowell, T. J., and D. Rees (1983), Derivation of a conservative equation for mean molecular weight for a two constituent gas within a three-dimensional, time-dependent model of the thermosphere, *Planet. Space Sci.*, *31*, 1209.

Hedin, A. E. (1987), MSIS-86 thermospheric model, *J. Geophys. Res.*, *92*(A5), 4649–4662.

Hines, C. O. (1967), On the nature of traveling ionospheric disturbances launched by low-altitude nuclear explosions, *J. Geophys. Res.*, *72*(7), 1877–1882.

Holton, J. R. (1992), An introduction to dynamic meteorology, International geophysics series, 3rd ed. Academic Press, San Diego, Calif.

Killeen, T. L., and R. G. Roble (1988), Thermosphere dynamics: Contributions from the first 5 years of the dynamics explorer program, *Rev. Geophys.*, *26*, 329–367.

Ma, T.-Z., and R. W. Schunk (1995), Effect of polar cap patches on the polar thermosphere, *J. Geophys. Res.*, *100*(A10), 19,701–19,713.

Rees, D., and T. J. Fuller-Rowell (1988), Understanding the transport of atomic oxygen in the thermosphere using a numerical global thermospheric model, *Plan. Space Sci.*, *36*, 935.

Rees, D., and T. J. Fuller-Rowell (1990), Numerical simulations of the seasonal/latitudinal variations of atomic oxygen and nitric oxide in the lower thermosphere and mesosphere, *Adv. Space Res.*, *10*(6), 83–102.

Richmond, A. D. (1992), Assimilative mapping of ionospheric electrodynamics, *Adv. Space Res.*, *12*, 59.

Ridley, A. J., Y. Deng, and G. Toth (2006), The global ionosphere-thermosphere model, *J. Atmos. Sol.-Terr. Phys.*, *68*, 839.

Rishbeth, H., I. C. F. Müller-Wodarg, L. Zou, T. J. Fuller-Rowell, G. H. Millward, R. J. Moffett, D. W. Idenden, and A. D. Aylward (2000), Annual and semiannual variations in the ionospheric F2-layer: II. Physical discussion, *Ann. Geophys.*, *18*, 945–956.

Roble, R. G., E. C. Ridley, A. D. Richmond, and R. E. Dickinson (1988), A coupled thermosphere/ionosphere general circulation model, *Geophys. Res. Lett.*, *15*(12), 1325–1328.

Y. Deng and W. Wang, High Altitude Observatory, National Center for Atmospheric Research, UCAR 1850 Table Mesa Drive, Boulder, CO 80305, USA. (ydeng@ucar.edu; wbang@ucar.edu)

A. J. Ridley, Center for Space Environment Modeling, University of Michigan, 2455 Hayward Street, Ann Arbor, MI 48109-2143, USA. (ridley@umich.edu)